Fluorescence Quenching by Nucleotides of the Plasma Membrane H^+-ATPase from *Kluyveromyces lactis*[†]

José G. Sampedro,*[,‡] Yadira G. Ruiz-Granados,[§] Hugo Nájera,[‡] Alfredo Téllez-Valencia,[||] and Salvador Uribe[§]

Área Académica de Nutrición and Area Ácadémica de Farmacia, ICSA Universidad Autónoma del Estado de Hidalgo, Abasolo 600 Colonia Centro, CP 42000, Pachuca, México, and Instituto de Fisiología Celular, Universidad Nacional Autónoma de México, AP 70-242, CP 04510, México

Received January 4, 2007; Revised Manuscript Received February 9, 2007

ABSTRACT: The yeast plasma membrane H^+-ATPase isolation procedure was improved; a highly pure enzyme (90−95%) was obtained after centrifugation on a trehalose concentration gradient. H^+-ATPase kinetics was slightly cooperative: Hill number = 1.5, $S_{0.5}$ = 800 μM ATP, and turnover number = 36 s^{-1}. In contrast to those of other P-type ATPases, H^+-ATPase fluorescence was highly sensitive to nucleotide binding; the fluorescence decreased 60% in the presence of both 5 mM ADP and AMP-PNP. Fluorescence titration with nucleotides allowed calculation of dissociation constants (K_d) from the binding site; K_d values for ATP and ADP were 700 and 800 μM, respectively. On the basis of amino acid sequence and homology model analysis, we propose that binding of the nucleotide to the N-domain is coupled to the movement of a loop β structure and to the exposure of the Trp505 residue located in the loop. The recombinant N-domain also displayed a large hyperbolic fluorescence quenching when ATP binds; however, it displayed a higher affinity for ATP (K_d = 100 μM). We propose for P-type ATPases that structural movements during nucleotide binding could be followed if a Trp residue is properly located in the N-domain. Further, we propose the use of trehalose in enzyme purification protocols to increase the purity and quality of the isolated protein and to perform structural studies.

The yeast plasma membrane H^+-ATPase (EC 3.6.3.6) is a member of the P-type ATPase family (*1*, *2*). The H^+-ATPase pumps protons out the cell, generating an inward ion gradient used for nutrient transport (*1*, *2*). Detailed structural studies for the plasma membrane H^+-ATPase from yeast and other sources are scarce. Efforts have been made in the *Neurospora crassa* H^+-ATPase, and its structure has been determined at 8 Å (*3*); comparison of the transmembrane α-helices of the *N. crassa* H^+-ATPase and the Ca^{2+}-ATPase has led Radresa et al. (*4*) to propose a specific path for protons (*4*).

The nucleotide sequence of the gene (*PMA1*) encoding the H^+-ATPase from *Saccharomyces cerevisiae*, *N. crassa*, and *Kluyveromyces lactis* is known (*1*, *5*, *6*). The numerous generated mutants have been useful in identifying the functional role of several amino acid residues (*7*). However, few structural studies have been performed limited mainly by the low purity of the isolated H^+-ATPase, probably due to the high structural instability of the native enzyme (*8*). Therefore, important questions remain to be answered, such as the coupling mechanism between ATP hydrolysis and proton transport. The native oligomeric state of the H-ATPase also remains to be determined (*7*).

In the H^+-ATPase catalytic cycle, it was proposed recently that ATP binding is followed by a 20° rotation of the nucleotide-binding domain (N-domain) that transfers the γ-phosphate to the Asp residue in the P-domain (*9*). Structural conformational changes upon substrate binding are a common process in enzymes (*10*), and intrinsic fluorescence is a physical parameter of choice for studying such structural movements (*11*), as fluorescence is highly sensitive to minimal environmental fluctuations. The H^+-ATPase structure contains 14 tryptophan residues, among which 13 of them are located at the transmembrane α-helices and solely one (W505) at the large cytoplasmic domain, specifically at the N-domain (*1*). Therefore, the appropriate location of W505 would be useful in studying nucleotide binding (ADP and ATP) monitored by fluorescence changes.

In this work, the method usually employed to isolate the plasma membrane H^+-ATPase from *S. cerevisiae* and *K. lactis* (*12*−*14*) was improved (90−95% pure enzyme was obtained). The structural instability of the H^+-ATPase was overcome by using, for the first time in a purification procedure, the disaccharide trehalose, a well-known protein stabilizer (*15*). The highly pure H^+-ATPase that was obtained made possible the nucleotide binding studies. The purified H^+-ATPase exhibited sigmoid kinetics (Hill number = 1.49) for ATP hydrolysis. Analysis of the N-domain amino acid sequence and its structural model revealed that W505 is located at the protein surface, specifically in the loop connecting two β-sheets (5 and 6). Nucleotide addition

[†] This research has been supported by Grants DGAPA/UNAM IN 227202 and CONACYT SEP-2004-C01-46537.

* To whom correspondence should be addressed. Telephone: +(5277) 1717 2000, ext. 5114. Fax: +(5277) 1717 2000, ext. 5111. E-mail: jg.sampedro@gmail.com.

[‡] Area Académica de Nutrición, ICSA Universidad Autónoma del Estado de Hidalgo.

[§] Universidad Nacional Autónoma de México.

[||] Área Académica de Farmacia, ICSA Universidad Autónoma del Estado de Hidalgo.

10.1021/bi700016v CCC: $37.00
Published on Web 04/17/2007

(5 mM) led to a large ATPase fluorescence quenching (60%); thus, titration of the binding site by nucleotides was possible and allowed the determination of the N-domain dissociation constants (K_d) for ADP and ATP. The same result was observed in the recombinant N-domain expressed in *Escherichia coli*. However, it exhibited a higher affinity for ATP, thus indicating the existence of an activated form of the H+-ATPase as suggested by others authors (*1*).

MATERIALS AND METHODS

Materials. Trehalose, glycerol, adenosine 5′-(β,γ-imido)-triphosphate (AMP-PNP), ADP sodium salt, and *N*-tetradecyl-*N*,*N*-dimethyl-3-ammonium-1-propane sulfonate (Zwittergent 3,14) were from Sigma Chemical Co. (St. Louis, MO). Coomassie brilliant blue R-250 and electrophoresis reagents were from Bio-Rad (Hercules, CA). Zymolyase-20T was from ICN Pharmaceuticals Inc. (Costa Mesa, CA). All other reagents were of the best quality commercially available.

Enzyme Purification. Plasma membranes were isolated as follows. *K. lactis* strain WM27 was grown in YPD at 30 °C for 20 h. The cells were harvested at the midlog phase and suspended in 1 M sorbitol (pH 7.0) containing zymolyase-20T (20 units/g of wet weight) at 30 °C for 1−2 h. Spheroplasts were detected by following spectrophotometrically the time-dependent decrease in turbidity (660 nm) of cell suspension aliquots (50 μL) in distilled water (3 mL). Yeast spheroplasts were disrupted by sonication at 4 °C, and plasma membranes were isolated by differential centrifugation. From the plasma membranes, the H+-ATPase was purified as described by Bowman and Slayman (*13*) and Guerra et al. (*14*), except that in the last purification step trehalose was used instead of glycerol. The plasma membranes were diluted to 2 mg/mL in buffer A [0.6 M KCl, 75 mM Tris, and 6 mM EDTA (pH 7.2)], 1 mM EGTA, and 0.1% (w/v) deoxycholate. The mixture was incubated under constant stirring at 4 °C for 10 min. Then, the solution was centrifuged at 100000*g* for 1 h. The pellet was resuspended to homogeneity in 10 mL of buffer B [0.3 M KCl, 25 mM Tris (pH 7.5), 45% (v/v) glycerol, and 2 mM EDTA], and the protein concentration was measured and adjusted to 5 mg/mL with buffer B. Azolectin (5 mg/mL) and Zwittergent 3,14 [0.85 (w/w) zwittergent:protein ratio] were added, and the suspension was homogenized and immediately centrifuged at 100000*g* for 1 h in a Beckman XL-100K refrigerated ultracentrifuge. The supernatant was carefully removed and poured onto a discontinuous trehalose concentration gradient formed by 4 mL aliquots of 50, 45, 40, 35, and 30% (w/v) trehalose in 10 mM Tris (pH 7.0), 1 mM EDTA, 0.1% deoxycholate, and 5 mg of azolectin/mL. The samples were centrifuged at 100000*g* for 14 h in a fixed angle rotor (60 Ti). On top of the 45% trehalose section, a white band was observed which contained the enriched plasma membrane H+-ATPase. This band was carefully removed and diluted 2-fold using 1 mM EGTA-Tris (pH 6.8). Then, the fractions were centrifuged at 100000*g* for 3 h, and the pellets were suspended in a small volume of 1 mM EGTA-Tris (pH 6.8) and kept at −70 °C until they were used. On SDS−PAGE, the 100 000 M_r band corresponding to the plasma membrane H+-ATPase was 90−95% (as determined by densitometry) of the total protein yield (Figure 1). The H+-ATPase specific activity at 25 °C was

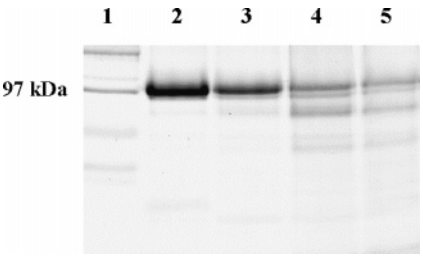

FIGURE 1: SDS−PAGE of the isolated plasma membrane H+-ATPase from *K. lactis*. The different fractions were obtained after centrifugation in the discontinuous trehalose gradient. The gel was stained with Coomassie blue as described in Materials and Methods: lane 1, molecular mass standards (from top to bottom), myosin (200 000 Da), β-galactosidase (116 250 Da), phosphorylase *b* (97 400 Da), serum albumin (66 200 Da), and ovalbumin (45 000 Da); lane 2, 45% trehalose fraction; lane 3, 40% trehalose fraction; lane 4, 35% trehalose fraction; and lane 5, 30% trehalose fraction. In lanes 2−5, the plasma membrane H+-ATPase protein corresponds to an M_r of 100 000 Da.

18.6 ± 0.3 μmol of P_i (mg of protein)$^{-1}$ min^{-1}. The protein concentration was determined using bovine serum albumin as a standard (*16*).

Measurement of H+-ATPase Activity. ATP saturation kinetics at 25 °C of the plasma membrane H+-ATPase was evaluated using an enzyme-coupled assay (*17*). The assay medium was 10 mM Pipes (pH 7.0), 80 mM KCl, 5 mM sodium azide, 5 mM phosphoenolpyruvate, 200 μM NADH, 12.5 IU of pyruvate kinase, 10.45 IU of lactic dehydrogenase, and 5 mM $MgCl_2$. Increasing concentrations of ATP (from 0.25 to 5.0 mM) were added as indicated. The assay solution was incubated at 25 °C for 10 min, and the H+-ATPase (4.3 μg of protein in 4 μL) was added to start the reaction. The absorbance decay at 340 nm was recorded continuously in a Shimadzu 2501PC spectrophotometer equipped with a thermostated cell. Initial rates for ATP hydrolysis (micromoles of ATP per milligram of protein per minute) were calculated from the slope of the linear portion of each trace, using a NADH extinction coefficient of 6200 M^{-1} cm^{-1}.

N-Domain Gene Synthesis, Expression, and Purification. The cDNA encoding the plasma membrane H+-ATPase N-domain was synthesized de novo by GeneScript Corp. (Piscatway, NJ), cloned in-frame into the *Eco*RI and *Not*I sites of the pGS-21a expression vector followed by *E. coli* BL-21(DE3) transformation. Expression and purification of the N-domain fused with both His_6-GST and His_6 were performed essentially as described by Pihlajamaa et al. (*18*) for the amino-terminal NC4 domain of human collagen IX.

Intrinsic Fluorescence Measurements. The fluorescence data of both the H+-ATPase and the recombinant N-domain were obtained at 25 °C in a Shimadzu RF 5301 spectrofluorophotometer equipped with a thermostated cell. The incubation mixture was 20 mM phosphate buffer (pH 6.8) with 5 mM $MgCl_2$ to which either the plasma membrane H+-ATPase or N-domain (final concentration of 0.1 μM) was added. After incubation for 5 min, the protein intrinsic fluorescence spectra were recorded between 300 and 450 nm using a 5 nm slit and an excitation wavelength of 290 and 280 nm for the H+-ATPase and N-domain, respectively. The ATPase fluorescence was titrated using either ADP or AMP-PNP, while the N-domain was titrated using either ADP or ATP. Titrations were performed by a stepwise increase of 0.5 mM nucleotide (2 μL additions from

a 0.5 M stock solution), and after each addition, the sample was incubated for 1 min and the fluorescence spectra were obtained. Fluorescence spectra were corrected for both dilution and an inner filter effect (*19*).

Data Analysis. Initial rates for ATP hydrolysis were calculated at different ATP concentrations from the slope of the linear portion of NADH absorbance decay (*20*). The observed sigmoid dependence of the rate of ATP hydrolysis on substrate concentration was analyzed, fitting the data to the Hill equation (eq 1) by nonlinear regression using the iterative software Origin 6.0 (Northampton, MA).

$$v = \frac{V_{max} S^n}{S_{0.5}{}^n + S^n} \quad (1)$$

where v is the initial rate, V_{max} is the maximum velocity for ATP hydrolysis, S is the ATP concentration, $S_{0.5}$ is the ATP concentration when $v = 0.5V_{max}$, and n is the Hill number.

The H^+-ATPase and N-domain steady state fluorescence intensities at 325 nm were plotted versus nucleotide concentration. Fluorescence data were fitted to eq 2 by nonlinear regression as described for other nucleotide binding proteins (*21*). Equation 2 describes the interaction of the substrate with a single binding site.

$$F_0 - F = \frac{\Delta F_{max} S}{K_d + S} \quad (2)$$

where $F_0 - F$ represents the quenching of the steady state fluorescence at 325 nm (the maximum peak) at a given nucleotide concentration S, ΔF_{max} is the maximum change in fluorescence intensity induced by substrate binding, and K_d is the constant for dissociation of the nucleotide from the binding site.

RESULTS AND DISCUSSION

In available isolation methods, the yeast plasma membrane H^+-ATPase is purified using a concentration gradient of glycerol or sucrose at the last purification step (*3*, *7*, *9*). However, contaminating proteins with a lower molecular mass (<100 kDa) are always present, affecting ATPase purity (*12*−*14*). It has been reported that the nonreducing sugar trehalose protects the native conformation of proteins against structural damage when subjected to harsh environmental conditions (*8*, *15*). Therefore, the use of trehalose in protein purification protocols might improve protein quality, e.g., preventing protein damage (inactivation or unfolding) or subunit dissociation, when oligomeric proteins are purified. In this work, the plasma membrane H^+-ATPase from *K. lactis* was purified using a trehalose gradient instead of the usual glycerol gradient (*12*, *14*). After centrifugation, a white band was observed in the 45% trehalose fraction. This was carefully collected, centrifuged, and resuspended in EGTA-Tris (pH 7.0) and the amount of protein quantified. Via SDS−PAGE, the plasma membrane H^+-ATPase was observed as a unique band of 100 kDa (Figure 1). The protein purity was between 90 and 95% as determined by densitometry (result not shown). The ATPase activity at 25 °C was 18.6 μmol of ATP (mg of protein)$^{-1}$ min^{-1}. Other trehalose fractions were also collected but with decreased ATPase purity; they displayed ATPase activity according to their H^+-ATPase content as follows: 40% trehalose fraction, 16.0 μmol of ATP (mg of protein)$^{-1}$ min^{-1}; 35% trehalose, 9.3 μmol of ATP (mg of protein)$^{-1}$ min^{-1}; and 30% trehalose, negligible ATPase activity.

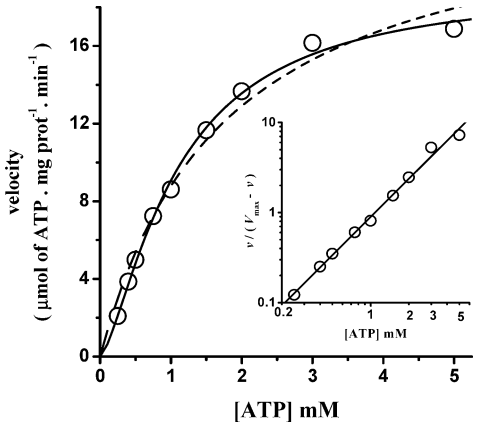

FIGURE 2: Enzyme kinetics of the plasma membrane H^+-ATPase at 25 °C. The initial rate for ATP hydrolysis was measured using an enzyme-coupled assay as described in Materials and Methods. The reaction was started by adding the enzyme and following the NADH absorbance decay at 340 nm. The data were fitted by nonlinear regression to the Hill equation (eq 1), where $n = 1.49$ (—) and 1 (- - -). The inset shows a Hill plot of the kinetic data; slope = $n = 1.48 \pm 0.02$. The data are the mean of three experiments where standard deviations are less than 5%.

In agreement with previous reports (*20*), the isolated plasma membrane H^+-ATPase exhibited sigmoid ATP saturation kinetics at 25 °C (Figure 2). The ATPase kinetic data fitted well to the Hill equation by nonlinear regression (eq 1). The calculated kinetic parameters were as follows: $V_{max} = 17.0 \pm 0.16$ μmol of ATP (mg of protein)$^{-1}$ min^{-1}, $S_{0.5} = 790 \pm 20$ μM ATP, and $n = 1.49 \pm 0.05$. H^+-ATPase cooperativity was further evidenced in the Hill plot (Figure 2, inset). The $S_{0.5}$ and the Hill number (n) were similar to those reported for the *S. cerevisiae* and *N. crassa* H^+-ATPases (*2*, *5*). The calculated turnover number for the purified H^+-ATPase was 36 s^{-1} and was similar to those reported for the Na,K-ATPase from different sources (*22*).

The binding of substrates (ADP and ATP) in the H^+-ATPase was studied by analyzing intrinsic fluorescence changes in the protein. The nonhydrolyzable ATP analogue AMP-PNP was used to prevent ATPase turnover (*11*). AMP-PNP and ATP are remarkably similar in size and shape; they differ solely in the protonation state of the γ-phosphate (*23*). The H^+-ATPase fluorescence spectra exhibited a maximum emission peak at 325 nm (Figure 3A) upon excitation at 290 nm. The H^+-ATPase fluorescence was largely quenched by increasing concentrations of both ADP (Figure 3A) and AMP-PNP (Figure 4A). Both AMP-PNP and ADP binding induced the same degree of fluorescence quenching. NMR studies of the isolated N-domain from Na,K-ATPase have shown that ADP and ATP are bound mainly through the base and sugar moieties, through a direct interaction with F, K, A, and L residues and leaving the phosphate groups exposed to the solvent, while an asparagine residue interacts with either the γ-phosphate of ATP or the β-phosphate of ADP to stabilize the complex (*24*). The fluorescence change induced by the binding of both nucleotides was the highest observed to date for a P-type ATPase; i.e., the ATPase fluorescence decreased 60% in the presence of 5 mM

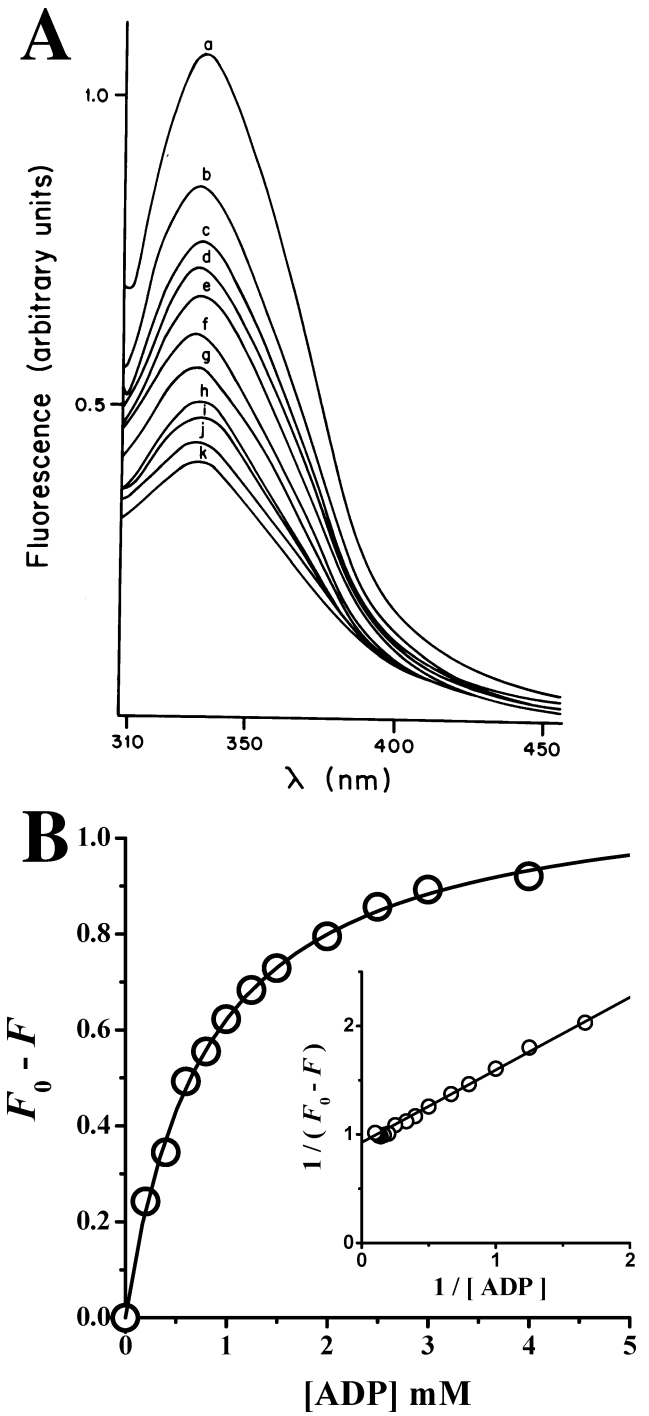

FIGURE 3: H+-ATPase fluorescence quenching by ADP binding. The isolated H+-ATPase (0.1 μM) was suspended in 20 mM phosphate buffer (pH 6.8) and 5 mM $MgCl_2$. The H+-ATPase fluorescence spectra were recorded (300−450 nM) after addition of nucleotide by exciting the protein at 290 nm. (A) H+-ATPase fluorescence spectra in the presence of different concentrations of ADP: (a) 0, (b) 0.5, (c) 1.0, (d) 1.5, (e) 2.0, (f) 2.5, (g) 3.0, (h) 3.5, (i) 4.0, (j) 4.5, and (k) 5.0 mM. (B) Plot of the H+-ATPase fluorescence intensity change (at 325 nm) vs ADP concentration. The line is the result of fitting the data by nonlinear regression to eq 2. The inset is a double-reciprocal plot. The calculated dissociation constant (K_d) value for ADP was 800 ± 30 μM. The fluorescence spectra and data points are the mean of three experiments; standard deviations were less than 5%.

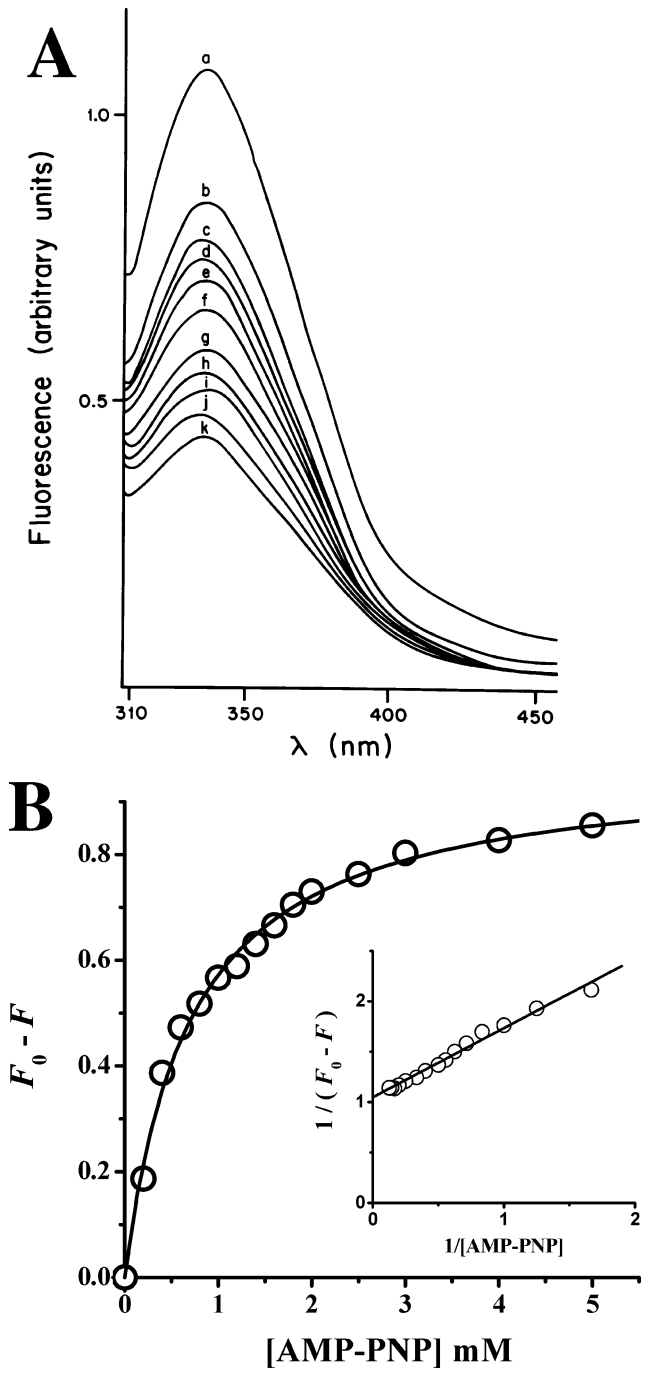

FIGURE 4: H+-ATPase fluorescence quenching by AMP-PNP binding. Experimental conditions as in Figure 3. (A) H+-ATPase fluorescence spectra in the presence of different concentrations of AMP-PNP: (a) 0, (b) 0.5, (c) 1.0, (d) 1.5, (e) 2.0, (f) 2.5, (g) 3.0, (h) 3.5, (i) 4.0, (j) 4.5, and (k) 5.0 mM. (B) Plot of the H+-ATPase fluorescence intensity change (at 325 nm) vs AMP-PNP concentration. The line was the result of fitting the data by nonlinear regression to eq 2. The inset is a double-reciprocal plot. The calculated dissociation constant (K_d) for AMP-PNP was 700 ± 30 μM. The fluorescence spectra and data points are the mean of three experiments; standard deviations were less than 5%.

nucleotide (Figures 3A and 4A) as compared to the fluorescence variation between 1 and 4% observed for the Ca^{2+}- and Na,K-ATPases (*11*, *25*, *26*).

H+-ATPase fluorescence quenching at 325 nm exhibited saturation hyperbolic dependence on both ADP and AMP-PNP concentrations. The data fitted well to eq 2 by nonlinear regression (Figures 3B and 4B). A straight line was formed in a double-reciprocal plot (Figures 3B and 4B, inset). AMP-PNP exhibited a higher affinity than ADP for the binding site as expected; the calculated dissociation constants (K_d)

H^+-ATPase *S pombe*	449-486	**F**DPVS**K**KVTAYVQAPDGTR ITCV**KGAP**L**W**VLKTVE EDH
H^+-ATPase *S cerevisiae*	451-488	**F**DPVS**K**KVTAVVESPEGER IVCV**KGAP**LFVLKTVE EDH
H^+-ATPase *K lactis*	432-469	**F**DPVS**K**KVTAIVESPEGER IICV**KGAP**LFVLKTVE EEH
H^+-ATPase *N crassa*	451-488	**F**DPVS**K**KVVAVVESPQGER ITCV**KGAP**LFVLKTVE EDH
Ca^{2+}-ATPase	487-535	**F**SRDR**K**SMSVYCSPAKSSRAAVGNKMFV**KGAP**EGVIDRCNYVRVGTTRV
Na,K-ATPase	482-528	**F**NSTN**K**YQLSIHKNPNASEP KHLLVM**KGAP**ERILDRCSSILLHGKEQ
H^+-ATPase *S pombe*	487-527	PIPEDVLSAYKDKVGDLAS RG Y**R**S**L**GVA RKIEGQH**W**EIMGI
H^+-ATPase *S cerevisiae*	489-529	PIPEDVHENYENKVAELAS RG F**RAL**GVA RKRGEGH**W**EILGV
H^+-ATPase *K lactis*	470-510	PIPEDVRENYENKVAELAS RG F**RAL**GVA RKRGEGH**W**EILGV
H^+-ATPase *N crassa*	489-529	PIPEEVDQAYKNKVAEFAT RG F**R**S**L**GVA RKRGEGS**W**EILGI
Ca^{2+}-ATPase	536-579	PMTGPVKEKILSVIKE**W**GTGRDTL**R**C**L**ALATRDTPPKREEMVLD
Na,K-ATPase	529-570	PLDEELKDAFQNAYLELGGLGE **RVL**GFCHLLLPDEQFPEGFQ

FIGURE 5: Amino acid sequence alignment of the nucleotide binding site. The amino acid sequences involved in nucleotide binding (*24*) in P-type ATPases from different species were aligned using the GENESTREAM network server (IGH, Montpellier, France). The highly conserved residues involved in nucleotide binding (F, K, A, R, and L) or pocked structure formation (K, G, and P) are shown in bold. The Na,K-ATPase (PDB entry 1MO7) sequence was used for alignment. Trp residues are bold and underlined.

for ADP and AMP-PNP were 800 ± 30 and 700 ± 30 μM, respectively. The substrate affinity for the active site was in agreement with the kinetic parameters for catalysis; $S_{0.5}$ was similar to the K_d for ATP.

The H^+-ATPase from *K. lactis* contains 14 Trp residues, and 13 of these are located at the transmembrane domain (TM) α-helices, and only one is located in the cytoplasmic nucleotide-binding domain (N-domain) (*1*, *4*, *6*). In the *K. lactis* N-domain amino acid sequence, W505 is located downstream from the highly conserved residues involved in nucleotide binding and pocket structure formation (F, K, K, G, A, P, R, and L) (Figure 5). The crystal structure of the H^+-ATPase still remains to be determined. However, a three-dimensional model is available (*9*), where W505 is located in the large disordered loop linking β-sheets 5 and 6 (β5−loop−β6) (Figure 6). In the Na,K-ATPase N-domain, it was proposed that the β6 structure performs a movement to close the nucleotide binding site (*24*); β6 changes from a bent to a straight structure which leads to a slight movement in the loop linking to β5. Therefore, in the N-domain, H^+-ATPase fluorescence variations upon nucleotide binding probably result from W505 environmental change (Figure 6). In contrast, in other P-ATPases where the N-domain Trp residue is completely buried or absent (*24*, *27*), either ADP or ATP binding induces negligible fluorescence changes (1−6%) (*25*, *26*, *28*).

The possibility that any of the 13 tryptophan residues at the TM could participate in fluorescence quenching was not excluded. Therefore, a gene (*NDPMA1*) encoding solely the N-domain H^+-ATPase was synthesized and cloned in the pGS-21a expression plasmid. The N-domain was purified to homogeneity by sequentially using affinity columns of Ni-Sepharose and GST-Prep^{MR}. The intrinsic fluorescence of the N-domain (which contains only a tryptophan residue, W505) was highly sensitive to ATP binding (Figure 7, inset); an 80% decrease in fluorescence was observed in the presence of 1 mM ATP, 20% higher than that observed in the H^+-ATPase. Saturation kinetics was also hyperbolic, allowing the fitting to eq 2 by nonlinear regression (Figure 7). The N-domain exhibited higher ATP affinity

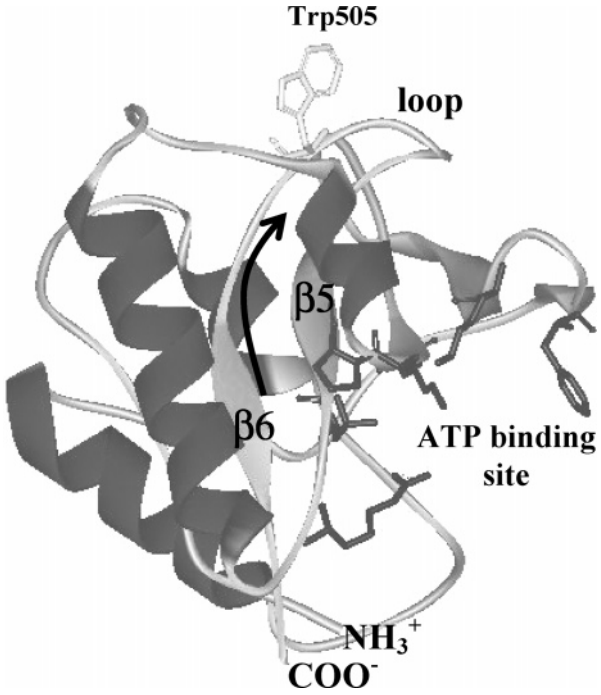

FIGURE 6: H^+-ATPase N-domain three-dimensional model. The *N. crassa* plasma membrane H^+-ATPase structural model (PDB entry 1MHS) built by Kühlbrandt et al. (*9*) was modified to show only the N-domain. The highly conserved amino acid residues involved in ATP binding are shown as sticks. The Trp505 residue is located at the loop linking structures 5β and 6β. The arrow shows the proposed loop 6β movement performed during nucleotide binding.

(K_d = 101 ± 7 μM) than in the whole H^+-ATPase protein (K_d = 700 ± 30 μM). This result supports the proposal of the existence of an activated state for the H^+-ATPase (*1*). The N-domain mutant lacking the Trp residue did not exhibit a fluorescence signal (results not shown).

P-Type ATPase structural studies have been performed mainly with the Na,K-ATPase and Ca^{2+}-ATPase from mammals (*27*, *29*). Conformational changes followed by intrinsic fluorescence have been largely scarce in these enzymes, mainly due to the absence of an adequately located

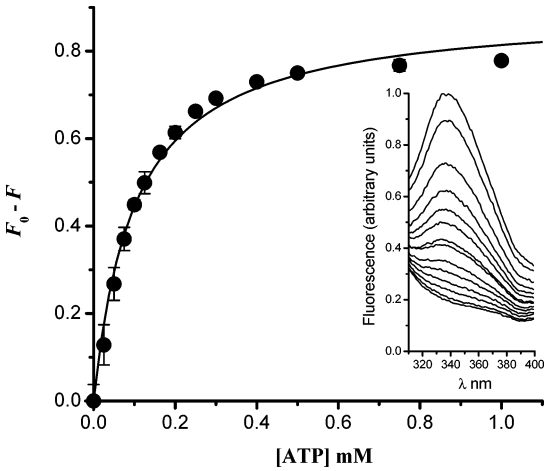

FIGURE 7: N-Domain fluorescence quenching by ATP binding. Experimental conditions as in Figure 3. The line was the result of fitting the data by nonlinear regression to eq 2. The inset shows the N-domain fluorescence spectra in the presence of different concentrations of ATP. The calculated dissociation constant (K_d) for ATP was 100.1 ± 7 μM. The fluorescence spectra and data points are the mean of three experiments; standard deviations were less than 5%.

Trp residue. Therefore, fluorescent nucleotides (TNP-ATP or Tb-FTP) or fluorescent covalent label probes must be used to perform studies on binding of the substrate to the N-domain (*30*−*32*). The use of trehalose (a membrane and protein stabilizer) in the H+-ATPase purification protocol improved the purity of the isolated protein. Both the highly pure H+-ATPase and the identification by molecular modeling of W505 (located at the motile structure β6 loop) allowed the study of binding of the substrate to H+-ATPase as monitored by fluorescence changes in the whole protein and confirmed in the isolated N-domain.

ACKNOWLEDGMENT

Dr. Antonio Peña (Instituto de Fisiología Celular, Universidad Nacional Autónoma de México) provided us with equipment, reagents, and advice for performing some experiments. We are thankful for the technical assistance of Nallely Cabrera, Andres Rojas-Hernandez, and Ramón Mendez from the Instituto de Fisiología Celular, Universidad Nacional Autónoma de México.

REFERENCES

1. Serrano, R., Kielland-Brandt, M. C., and Fink, G. R. (1986) Yeast plasma membrane ATPase is essential for growth and has homology with ($Na^{2+}K^+$), K^+- and Ca^{2+}-ATPases, *Nature 319*, 689−693.
2. Nakamoto, R. K., and Slayman, C. W. (1989) Molecular properties of the fungal plasma-membrane [H+]-ATPase, *J. Bioenerg. Biomembr. 21*, 621−632.
3. Auer, M., Scarborough, G. A., and Kühlbrandt, W. (1999) Surface crystallisation of the plasma membrane H+-ATPase on a carbon support film for electron crystallography, *J. Mol. Biol. 287*, 961−968.
4. Radresa, O., Ogata, K., Wodak, S., Ruysschaert, J. M., and Goormaghtigh, E. (2002) Modeling the three-dimensional structure of H+-ATPase of *Neurospora crassa*, *Eur. J. Biochem. 269*, 5246−5258.
5. Rao, R., Nakamoto, R. K., Verjovski-Almeida, S., and Slayman, C. W. (1992) Structure and function of the yeast plasma-membrane H+-ATPase, *Ann. N.Y. Acad. Sci. 671*, 195−203.
6. Miranda, M., Ramirez, J., Peña, A., and Coria, R. (1995) Molecular cloning of the plasma membrane H+-ATPase from *Kluyveromyces lactis*: A single nucleotide substitution in the gene confers ethidium bromide resistance and deficiency in K^+ uptake, *J. Bacteriol. 177*, 2360−2367.
7. Morsomme, P., Slayman, C. W., and Goffeau, A. (2000) Mutagenic study of the structure, function and biogenesis of the yeast plasma membrane H+-ATPase, *Biochim. Biophys. Acta 1469*, 33−57.
8. Sampedro, J. G., Cortés, P., Muñoz-Clares, R., Fernández, A., and Uribe, S. (2001) Thermal inactivation of the plasma membrane H+-ATPase from *Kluyveromyces lactis*. Protection by trehalose, *Biochim. Biophys. Acta 1544*, 64−73.
9. Kühlbrandt, W., Zeelen, J., and Dietrich, J. (2002) Structure, mechanism, and regulation of the *Neurospora* plasma membrane H+-ATPase, *Science 297*, 1692−1696.
10. Hammes, G. G. (2002) Multiple conformational changes in enzyme catalysis, *Biochemistry 41*, 8221−8228.
11. Dupont, Y., Guillain, F., and Lacapere, J. J. (1988) Fluorimetric detection and significance of conformational changes in Ca^{2+}-ATPase, *Methods Enzymol. 157*, 206−219.
12. Bowman, B. J., and Slayman, C. W. (1979) The effects of vanadate on the plasma membrane ATPase of *Neurospora crassa*, *J. Biol. Chem. 254*, 2928−2934.
13. Bowman, B. J., Blasco, F., and Slayman, C. W. (1981) Purification and characterization of the plasma membrane ATPase of *Neurospora crassa*, *J. Biol. Chem. 256*, 12343−12349.
14. Guerra, G., Uribe, S., and Pardo, J. P. (1995) Reactivity of the H+-ATPase from *Kluyveromyces lactis* to sulfhydryl reagents, *Arch. Biochem. Biophys. 321*, 101−107.
15. Sampedro, J. G., Guerra, G., Pardo, J. P., and Uribe, S. (1998) Trehalose-mediated protection of the plasma membrane H+-ATPase from *Kluyveromyces lactis* during freeze-drying and rehydration, *Cryobiology 37*, 131−138.
16. Lowry, O. H., Nira, J. N., Rosebrough, J., Farr, A. L., and Randall, R. J. (1951) Protein measurement with the Folin phenol reagent, *J. Biol. Chem. 193*, 265−275.
17. Anderson, K. W., and Murphy, A. J. (1983) Alterations in the structure of the ribose moiety of ATP reduce its effectiveness as a substrate for the sarcoplasmic reticulum ATPase, *J. Biol. Chem. 258*, 14276−14278.
18. Pihlajamaa, T., Lankinen, H., Ylostalo, J., Valmu, L., Jaalinoja, J., Zaucke, F., Spitznagel, L., Gosling, S., Puustinen, A., Morgelin, M., Peranen, J., Maurer, P., Ala-Kokko, L., and Kilpelainen, I. (2004) Characterization of recombinant amino-terminal NC4 domain of human collagen IX: Interaction with glycosaminoglycans and cartilage oligomeric matrix protein, *J. Biol. Chem. 279*, 24265−24273.
19. Ward, L. D. (1985) Measurement of ligand binding to proteins by fluorescence spectroscopy, *Methods Enzymol. 117*, 400−414.
20. Sampedro, J. G., Muñoz-Clares, R. A., and Uribe, S. (2002) Trehalose-mediated inhibition of the plasma membrane H+-ATPase from *Kluyveromyces lactis*: Dependence on viscosity and temperature, *J. Bacteriol. 184*, 4384−4391.
21. Liu, R., and Sharom, F. J. (1997) Fluorescence studies on the nucleotide binding domains of the P-glycoprotein multidrug transporter, *Biochemistry 36*, 2836−2843.
22. Lupfert, C., Grell, E., Pintschovius, V., Apell, H. J., Cornelius, F., and Clarke, R. J. (2001) Rate limitation of the Na^{2+},K^+-ATPase pump cycle, *Biophys. J. 81*, 2069−2081.
23. von Germar, F., Barth, A., and Mantele, W. (2000) Structural changes of the sarcoplasmic reticulum Ca^{2+}-ATPase upon nucleotide binding studied by Fourier transform infrared spectroscopy, *Biophys. J. 78*, 1531−1540.
24. Hilge, M., Siegal, G., Vuister, G. W., Guntert, P., Gloor, S. M., and Abrahams, J. P. (2003) ATP-induced conformational changes of the nucleotide-binding domain of Na,K-ATPase, *Nat. Struct. Biol. 10*, 468−474.
25. Dupont, Y., Chapron, Y., and Pougeois, R. (1982) Titration of the nucleotide binding sites of sarcoplasmic reticulum Ca^{2+}-ATPase with 2′,3′-O-(2,4,6-trinitrophenyl) adenosine 5′-triphosphate and 5′-diphosphate, *Biochem. Biophys. Res. Commun. 106*, 1272−1279.
26. Lacapere, J. J., Bennett, N., Dupont, Y., and Guillain, F. (1990) pH and magnesium dependence of ATP binding to sarcoplasmic reticulum ATPase. Evidence that the catalytic ATP-binding site consists of two domains, *J. Biol. Chem. 265*, 348−353.
27. Toyoshima, C., Nakasako, M., Nomura, H., and Ogawa, H. (2000) Crystal structure of the calcium pump of sarcoplasmic reticulum at 2.6 Å resolution, *Nature 405*, 647−655.

28. Dupont, Y., and Leigh, J. B. (1978) Transient kinetics of sarcoplasmic reticulum Ca^{2+},Mg^{2+}-ATPase studied by fluorescence, *Nature 273*, 396−398.
29. Hakansson, K. O. (2003) The crystallographic structure of Na,K-ATPase N-domain at 2.6 Å resolution, *J. Mol. Biol. 332*, 1175−1182.
30. Watanabe, T., and Inesi, G. (1982) The use of 2′,3′-O-(2,4,6-trinitrophenyl) adenosine 5′-triphosphate for studies of nucleotide interaction with sarcoplasmic reticulum vesicles, *J. Biol. Chem. 257*, 11510−11516.
31. Ronjat, M., Lacapere, J. J., Dufour, J. P., and Dupont, Y. (1987) Study of the nucleotide binding site of the yeast *Schizosaccharomyces pombe* plasma membrane H^+-ATPase using formycin triphosphate-terbium complex, *J. Biol. Chem. 262*, 3146−3153.
32. Fonseca, M. M., Scofano, H. M., Carvahlo-Alves, P. C., Barrabin, H., and Mignaco, J. A. (2002) Conformational changes of the nucleotide site of the plasma membrane Ca^{2+}-ATPase probed by fluorescence quenching, *Biochemistry 41*, 7483−7489.

BI700016V